SAND20XX-XXXXR
LDRD PROJECT NUMBER: 177861
LDRD PROJECT TITLE: Exploring Charge Transport in Guest Molecule Infiltrated $Cu_3(BTC)_2$ Metal Organic Framework
PROJECT TEAM MEMBERS: A. A. Talin, F. Leonard, V. Stavila, M. D. Allendorf

ABSTRACT:

The goal of this Exploratory Express project was to expand the understanding of the physical properties of our recently discovered class of materials consisting of metal-organic frameworks with electroactive 'guest' molecules that together form an electrically conducting charge-transfer complex (molecule@MOF). Thin films of $Cu_3(BTC)_2$ were grown on fused silica using solution step-by-step growth and were infiltrated with the molecule tetracyanoquinodimethane (TCNQ). The infiltrated MOF films were extensively characterized using optical microscopy, scanning electron microscopy, Raman spectroscopy, electrical conductivity, and thermoelectric properties. Thermopower measurements on TCNQ@$Cu_3(BTC)_2$ revealed a positive Seebeck coefficient of ~400 μV/k, indicating that holes are the primary carriers in this material. The high value of the Seebeck coefficient and the expected low thermal conductivity suggest that molecule@MOF materials may be attractive for thermoelectric power conversion applications requiring low cost, solution-processable, and non-toxic active materials.

INTRODUCTION:

Metal-organic frameworks (MOFs) are extended, crystalline compounds consisting of metal ions interconnected by organic ligands, forming scaffolding-like structures that are sometimes referred to as "molecular tinker toys". [1] These highly porous materials have attracted considerable attention for potential applications in gas storage, separation and catalysis. [2] The combination of crystallinity and remarkable synthetic versatility makes MOFs attractive for electronic applications, as well, where the long range order of MOFs should lead to higher charge mobility, while their chemical tunability could be used to control the carrier type and the bandgap. Achieving electrical conductivity will significantly widen the potential application space for MOFs, including electronic devices (i.e. FETs) for flexible electronics, energy storage and conversion devices, and chemical sensors. Most MOFs, however, are electrical insulators due to the non-conjugated character of the organic ligands and poor overlap between their π orbitals and the d orbitals of the metal ions. Recently, several MOFs with electrical conductivity ranging from ~10^{-7} S/cm to ~10^{1} S/cm have been demonstrated[3]. In purely organic polymers conductivity is directly related to having a highly conjugated π bond network, which allows facile charge transport along individual chains. Closely packing these chains in crystalline domains enhances their p-electron coupling and leads to true band transport and higher mobility. Similarly for MOFs, conductivity along specific bonding directions is enhanced by using aromatic bridging ligands that form more covalent interactions with the metal ions (the 'through-bond' approach). Alternatively, electroactive ligands may be π-stacked in 1-dimensional channels leading to conductivity along the packing direction. Examples of 'through-bond' conducting MOFs include frameworks with metal ion−thiophenoxide linkages wherein the sulfur

atoms interact with the same d orbital of metal thus promoting charge delocalization along the (−M−S−) chain [3b], Cu-Ni MOFs with redox-active linkers,[4] and Fe-triazolate frameworks.[5] Examples of MOFs and covalent organic frameworks (COFs) where conductivity primarily arises from π-stacking of electroactive linkers include assemblies of pyrene and triphenylene, porphyrine, phthalocyanins, tetrathiafulvalene, and hexaaminotriphenylene [3d]. An alternative approach is to introduce a redox-active guest molecule that bridges neighboring metal centers thus promoting charge delocalization and electrical conductivity. Using this 'molecule@MOF' concept we recently demonstrated that the electrical conductivity of a $Cu_3(BTC)_2$ (BTC – benzene tricarboxylate) MOF, commonly known as HKUST-1 can be increased by >7 orders of magnitude with the introduction of the guest molecule TCNQ (tetracyanoquinodimethane).[6] Molecular cluster calculations indicated that TCNQ binds to two Cu(II) dimer units within the MOF pores, acting as a 'bridge' for electron transfer between these 'donor' and 'acceptor' sights. Indeed, partial charge transfer of ~0.3e^- between the TCNQ and the framework was confirmed by infrared and Raman spectroscopic measurements. Temperature dependent conductivity measurements indicated hopping carrier transport with a very low activation energy of ~0.04 eV. Herein we report on thermoelectric measurements TCNQ@$Cu_3(BTC)_2$ films which reveal a positive Seebeck coefficient of ~400 μV/K, indicating that the charge carriers in TCNQ@$Cu_3(BTC)_2$ are holes. The large magnitude of the Seebeck coefficient suggests that molecule@MOF materials may be promising for thermoelectric power conversion, particularly for applications requiring processing routes amenable to deposition over large area and complex shape substrates, mechanical flexibility, and utilizing low cost, earth abundant and non-toxic elements.

In addition to characterizing the thermoelectric properties of TCNQ@$Cu_3(BTC)_2$, we have explored the electrical and optical characteristics of two new molecule@MOF materials, BTT@$Cu_3(BTC)_2$ and TTF@$Cu_3(BTC)_2$. Both materials were found to be insulating as prepared. However, when illuminated with 325 nm a $\times 10^5$ increase in conductivity from $<10^{-8}$ S/cm to 10^{-3} cm/S was observed for BTT@$Cu_3(BTC)_2$. A similar response was observed for TTF@$Cu_3(BTC)_2$This is the first observation of photoconductivity in a molecule@MOF compound and is due to optical excitation of charge carriers.

.

DETAILED DESCRIPTION OF EXPERIMENT/METHOD:

$Cu_3(BTC)_2$ films with 200 nm nominal thickness were grown from the liquid phase on fused quartz substrates 19×19 mm^2, 0.55 mm thick according to a previously described recipe [7]. Briefly, the growth is performed using a custom reactor with precursors dissolved in ethanol introduced in a sequential manner, and separated by a pure ethanol 'cleaning' cycle. The growth has 'step-by-step' characteristics similar to those observed in atomic layer epitaxy and allows for excellent thickness control. Unfortunately, the growth is also very slow, with 24 hours typically necessary to deposit films with thickness exceeding 100 nm in thickness. Quartz and Si with thermally grown oxide of 100 nm in thickness were used as substrates. The substrates had pre-patterned Au pads with dimensions of 200 μm x 500 μm and with spacing of 85, 110, 135, and 160 μm which provided bottom electrical contacts to the MOF film. The thickness of the Au pads was 100 nm, with ~4 nm of Ti sticking layer. Prior to deposition the substrates were degreased in acetone and ethanol and exposed to UV-ozone to remove surface contaminants. After growth the specimens were dried under nitrogen stream. Grazing incidence XRD measurements and SEM imaging indicated polycrystalline $Cu_3(BTC)_2$ films with preferred

orientation along the (111) direction. Prior to infiltration, the residual solvent and precursors were removed by heating the samples at 180 ^{o}C in vacuum (~10^{-6} Torr) for a period of ~one hour. After activation, the samples were immediately transferred into a glass bottle container partially filled with a saturated solution of TCNQ in methanol. The specimen was held vertically in the glass vessel by side ridges such that only ~the lower half of the specimen was in contact with the methanol/TCNQ solution, as shown in Fig. 1a. The specimen was held in the TCNQ solution for ~24 hours, rinsed with methanol, and blown dry with nitrogen. Optical inspection was performed using a Leica high resolution microscope. Electrical conductivity was measured under DC bias using a computer controlled voltage/current source/measure source (National Instruments) with a current amplifier. The Au pads were contacted using Au tips with 1 μm radius controlled with manual micromanipulators. Voltage scan rate was 0.1 V/s for all measurements and the voltage range was generally -10 V to 10 V. Current-voltage measurements were collected at different pad separations and then repeated to ensure that the process of colleting I-V curves did not perturb the film (this process is sometimes referred to as 'forming'). Additional current-voltage measurements were collected by contacting the film directly with the Au coated probes, without the Au pads underneath.

Raman spectra were collected using a home built system equipped with a 532 nm excitation source (frequency doubled Nd:YAG), and an Acton research 2275 spectrometer. The laser is focused using an upright microscope. All spectra were collected with a 600 groove/mm grating and with ~1 mW of power at the sample focused into a spot that is ~2 μm in diameter. This is equivalent to ~3×10^{5} W/cm^{2}. Each spectrum represents an average of three spectra each collected over a period of 30 seconds. The effective spectral resolution of the Raman spectrometer with these settings is ~1 cm^{-1}. The Raman microscope also allows for visual inspection of the specimen. No visual changes such as discoloration were observed after collection of the Raman spectra, nor were there observable changes in the spectra themselves, indicating that the MOF films were not damaged by the laser illumination.

To determine the Seebeck coefficient, the specimen was placed onto a custom stage consisting of two Peltier heaters/coolers (TEC1-12710 TEC) which were used to establish a thermal gradient; the thermovoltage was then measured using a precision voltage meter (Agilent) while the local temperature was determined using an Inframeterics 760 IR thermal imaging camera. A schematic of the setup and a thermal image of the specimen are shown in Figs. 2a and 2b, respectively. The temperature was collected at positions 200 μm above and below the Au pads, to avoid the effect of the Au pads given the low emissivity value for Au, and the average of these two temperatures was recorded. The emissivity of the MOF film was experimentally determined to be 0.80.

Infiltration with BDT and TTF was performed by immersing an activated Cu3(BTC)2 coating on Si/SiO2 substrate into a methylene chloride solution saturated with the molecule of interest.

RESULTS:

The morphology and microstructure of $Cu_3(BTC)_2$ films grown using the automated layer-by-layer method has been described in detail elsewhere[7]. Briefly, the resulting films are polycrystalline with a preferred (111) orientation and grain size that ranges from tens of nanometers to ~1 μm depending on the film thickness and exact growth conditions. A cross section SEM image of a $Cu_3(BTC)_2$ film grown on a Si/SiO_2 substrate using the conditions in this study is shown in Fig. 1a. Immersion of the $Cu_3(BTC)_2$ coated quartz specimen into the TCNQ/methanol solution (yellow liquid in Fig. 1b) for ~24 hours resulted in the MOF film acquiring a deep blue-green color. The color of the TCNQ infiltrated $Cu_3(BTC)_2$ arises from a broad absorption band centered at ~690 nm due to a ligand-to-metal charge transfer transition occurring between the guest molecules and Cu^{2+} ions in the framework[6]. The infiltrated (region 'A') and non-infiltrated (region 'B') portions are separated by a 'boundary' area (region 'B' in Fig. 1c and 1d) that extends along the upper edges of the specimen where the TCNQ/methanol solution wicked up along the container ridges that were used to hold the specimen in a vertical position. Representative I-V measurements collected at the three regions are shown in Fig. 1e, where it can be seen that only region 'A' shows measurable conductivity. The conducting/insulating characteristic of the infiltrated/non-infiltrated regions can also be clearly seen in a low resolution scanning electron microscope (SEM) image of the specimen, where the insulating regions appear very bright due to charging under the electron beam (charging is generally not an issue when the MOF is deposited on conducting substrates such as Si or Si with a thin layer of SiO_2).

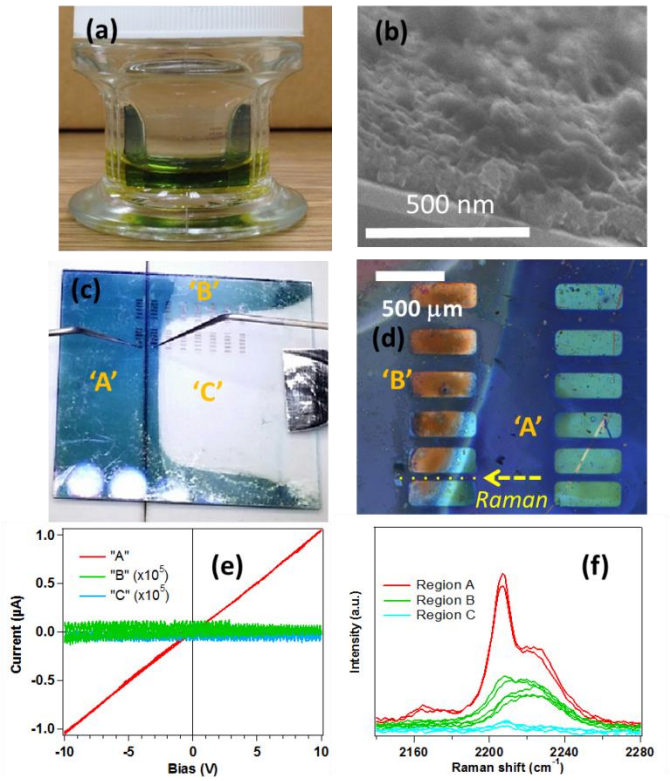

Figure 1 (a) The quartz substrate with 60 nm thick Cu3(BTC)2 MOF film is partially immersed into a saturated solution of TCNQ in methanol (b) SEM crossection of the MOF film (c) Optical image of the MOF film after infiltration with three distinct regions referenced in the text (d) Higher magnification of the same region indicating location of the microRaman spectra (e) I-V plots for the three regions indicated in (c). (f) Raman -C≡N vibrations for the three regions.

A series of μRaman spectra corresponding to the C≡N vibration (~2300 cm^{-1}) collected at locations indicated by the yellow dots in Figure 1d are shown in Fig. 1e. The C≡N stretching frequency in TCNQ salts is sensitive to

the degree of charge transfer[8]; since only two of the four C≡N groups are involved in bridging neighboring Cu^{2+} ions, the C≡N vibration in the infiltrated region is split into two peaks. Its higher intensity is likely due to a resonance effect since the infiltrated region has

substantial absorption at the Raman laser wavelength (532 nm). The downshifted C≡N peak can still be seen in region 'B', but its intensity is greatly diminished. In the transition region infiltration likely only occurred in the top surface of the MOF film, far from the Au contact pads. This may explain why the transition region remained insulating.

Resistance measurements as a function of temperature and Au pad separation (channel length) are shown in Fig. S3a. The linear I/V curves (Fig. 1f) and the linear increase in resistance with channel length are consistent with Ohmic conduction in TCNQ@$Cu_3(BTC)_2$. A plot of the conductivity versus 1/T is shown in Fig. S3b and yields an activation energy of 0.052 eV, slightly above the 0.040 eV activation barrier we previously reported for similarly prepared films on Si/SiO2 substrates.[6]

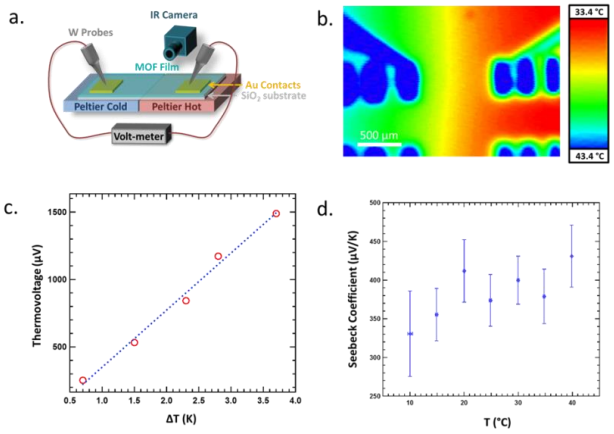

Figure 2 (a) Schematic of the setup used to measure the Seebeck coefficient. (b) Infrared camera image showing the temperature gradient across the MOF/quartz specimen. (c) Thermovoltage versus delta-T measured at 40 °C. (d) Seebeck coefficient measured as a function of temperature.

DISCUSSION:

Arrhenius-type temperature dependence of the conductivity with an activation barrier of 0.052 eV could, in principle, be explained by assuming that TCNQ@$Cu_3(BTC)_2$ is a semiconductor with an energy gap of ~0.10 eV. However, this assumption is inconsistent with the observed optical absorption band centered at ~700 nm, or with the results of our *ab initio* calculations which yield a gap of 1.76 eV between the HOMO orbitals localized mostly on the copper dimer groups (MOF SBUs) and the LUMO orbitals localized mostly on the TCNQ guests. An alternate explanation for the observed conductivity involves hopping of carriers between ground states associated with neighboring copper dimers bridged by TCNQ dimers. Observation of low activation energy for charge transfer in the ground state and optical absorption band in the visible range is fully consistent with our earlier classification of TCNQ@$Cu_3(BTC)_2$ as a Class II Robin-Day system[6, 9] A similar model was recently proposed to account for the thermally activated conduction in Berlin green (BG), the oxidized form of Prussian blue (PB)[10]. In the case of PB, conduction at room temperature only occurs once some of the low-spin C-coordinated Fe^{2+} ions are oxidized to Fe^{3+} to create empty states (holes) in the t_{2g} block, which Pajerowski et al associated with the 'valence band'[10]. In our case, oxidation of TCNQ@$Cu_3(BTC)_2$ is not necessary, since the e_g block of the approximately octahedrally split Cu^{2+} ions is already populated with only 3 d-electrons[11], i.e. there is already a 'hole' present. This explanation is an oversimplification, since copper dimers are not in true octahedral splitting. In fact, the d electrons on the two Cu^{2+} ions due interact leading to a splitting between a singlet and triplet states with an energy of 0.042 eV, in close agreement with our observed activation

energy for conduction. In other words, the necessary thermal activation may be the creation of an empty state in the Cu d-block electrons.

All-organic polymers require oxidative or reductive doping to create charge carriers, usually in form of polarons or bipolarons. Unless the polymers are doped, they are typically very poor conductors at room temperature. This is the result of Peierls distortion whereby the polymer chains break the symmetry associated with all the bonds being the same length (i.e. p-electrons evenly delocalized) to create lower and higher energy states and all of the available p-electrons fill the lower states with a substantial energy gap on the order of 1 eV between the filled and empty states. Introduction of an acid into the polymer removes some of the p-electrons leaving behind holes that are able to conduct electricity. The acid 'dopant' however, also substantially increase disorder leading to lower charge carrier diffusion length and lower mobility. Our resuts demonstrate that a conducting MOF can be prepared without the need for acid or base 'dopant'. Rather the conduction occurs as a result of the transition metal d band occupancy, which may or may not have empty states necessary for conduction.

Plots of thermovoltage versus ΔT measured at 40 ^{o}C and the Seebeck coefficient as a function of temperature are shown in Fig. 2c and 2d, respectively. The positive value of the Seebeck coefficient indicates that holes are the majority carrier type for TCNQ@$Cu_3(BTC)_2$. Therefore, the Fermi level lies either close to or within the valence band. This result is consistent with the model described above, i.e. that conduction occurs in the partially filled valence band consisting of the Cu^{2+} dimer SBUs. Band-like or metallic transport, however, is not observed due to insufficient coupling between the bridged MOF SBUs. Since the magnitude of the Seebeck coefficient is proportional to $d\left[\ln \sigma(E)/dE\right]_{E=E_F}$, where σ is the conductivity, the relatively high value of ~400 μV/K, implies that the Fermi level lies near the valence band edge, where the electronic density of states is expected to vary strongly with energy.

ANTICIPATED IMPACT:

This study is anticipated to impact both the fundamental science of charge transport in hybrid organic-inorganic polymers and the practical need for thermoelectric materials that operate at or near room temperature, that are made from earth-abundant and inexpensive materials, non-toxic, and which can be solution processed to cover large area and complex three dimensional shapes. Clearly, traditional inorganic thermoelectric materials such as bismuth telluride do not fit this description. Beyond thermoelectrics, conducting MOFs and molecule@MOFs represent completely new electronic materials with essentially unexplored and potentially useful properties. A manuscript based on this work and slated for submission to a high impact journal is currently being prepared. A full LDRD proposal focused on MOFs and molecule@MOFs was succesfful submitted to the Sandia LDRD office. Additionally, white papers are being submitted to ARPA-E in collaboration with Georgia Tech and MIT, as well as to DARPA in collaboration with MIT and PARC. In both proposals, electrically conducting molecule@MOF materials play a central role.

CONCLUSION:

We have measured a Seebeck coefficient of ~400 mV/K for the molecule@MOF material TCNQ@$Cu_3(BTC)_2$. The positive sign of the coefficient indicates that holes are the primary current carriers in TCNQ@$Cu_3(BTC)_2$ and the large value suggest that molecule@MOF materials are promising for thermoelectric energy conversion applications.

1. (a) Suh, M. P.; Park, H. J.; Prasad, T. K.; Lim, D.-W., Hydrogen Storage in Metal–Organic Frameworks. *Chem. Rev.* **2011,** *112* (2), 782-835; (b) Sumida, K.; Rogow, D. L.; Mason, J. A.; McDonald, T. M.; Bloch, E. D.; Herm, Z. R.; Bae, T.-H.; Long, J. R., Carbon Dioxide Capture in Metal–Organic Frameworks. *Chem. Rev.* **2011,** *112* (2), 724-781.
2. Lee, J.; Farha, O. K.; Roberts, J.; Scheidt, K. A.; Nguyen, S. T.; Hupp, J. T., Metal-organic framework materials as catalysts. *Chemical Society Reviews* **2009,** *38* (5), 1450-1459.
3. (a) D'Alessandro, D. M.; Kanga, J. R. R.; Caddy, J. S., Towards Conducting Metal-Organic Frameworks. *Australian J. Chem.* **2011,** *64* (6), 718-722; (b) Sun, L.; Miyakai, T.; Seki, S.; Dinca, M., Mn-2(2,5-disulfhydrylbenzene-1,4-dicarboxylate): A Microporous Metal-Organic Framework with Infinite (-Mn-S-)(infinity) Chains and High Intrinsic Charge Mobility. *Journal of the American Chemical Society* **2013,** *135* (22), 8185-8188; (c) Stavila, V.; Talin, A. A.; Allendorf, M. D., MOF-based electronic and opto-electronic devices. *Chemical Society reviews* **2014,** *43* (16), 5994-6010; (d) Sheberla, D.; Sun, L.; Blood-Forsythe, M. A.; Er, S.; Wade, C. R.; Brozek, C. K.; Aspuru-Guzik, A.; Dinca, M., High Electrical Conductivity in Ni-3(2,3,6,7,10,11-hexaiminotriphenylene)(2), a Semiconducting Metal-Organic Graphene Analogue. *Journal of the American Chemical Society* **2014,** *136* (25), 8859-8862.
4. Kobayashi, Y.; Jacobs, B.; Allendorf, M. D.; Long, J. R., Conductivity, Doping, and Redox Chemistry of a Microporous Dithiolene-Based Metal-Organic Framework. *Chemistry of Materials* **2010,** *22* (14), 4120-4122.
5. Gandara, F.; Uribe-Romo, F. J.; Britt, D. K.; Furukawa, H.; Lei, L.; Cheng, R.; Duan, X. F.; O'Keeffe, M.; Yaghi, O. M., Porous, Conductive Metal-Triazolates and Their Structural Elucidation by the Charge-Flipping Method. *Chem. Eur. J.* **2012,** *18* (34), 10595-10601.
6. Talin, A. A.; Centrone, A.; Ford, A. C.; Foster, M. E.; Stavila, V.; Haney, P.; Kinney, R. A.; Szalai, V.; El Gabaly, F.; Yoon, H. P.; LÃ©onard, F. o.; Allendorf, M. D., Tunable Electrical Conductivity in Metal-Organic Framework Thin-Film Devices. *Science* **2014,** *343* (6166), 66-69.
7. Stavila, V.; Volponi, J.; Katzenmeyer, A. M.; Dixon, M. C.; Allendorf, M. D., Kinetics and mechanism of metal-organic framework thin film growth: systematic investigation of HKUST-1 deposition on QCM electrodes. *Chemical Science* **2012,** *3* (5), 1531-1540.
8. Chappell, J. S.; Bloch, A. N.; Bryden, W. A.; Maxfield, M.; Poehler, T. O.; Cowan, D. O., DEGREE OF CHARGE-TRANSFER IN ORGANIC CONDUCTORS BY INFRARED-ABSORPTION SPECTROSCOPY. *Journal of the American Chemical Society* **1981,** *103* (9), 2442-2443.
9. Brunschwig, B. S.; Creutz, C.; Sutin, N., Optical transitions of symmetrical mixed-valence systems in the Class II–III transition regime. *Chemical Society Reviews* **2002,** *31*, 17.
10. Pajerowski, D. M.; Watanabe, T.; Yamamoto, T.; Einaga, Y., Electronic conductivity in Berlin green and Prussian blue. *Phys. Rev. B* **2011,** *83* (15).
11. Prestipino, C.; Regli, L.; Vitillo, J. G.; Bonino, F.; Damin, A.; Lamberti, C.; Zecchina, A.; Solari, P. L.; Kongshaug, K. O.; Bordiga, S., Local structure of framework Cu(II) in HKUST-1 metallorganic framework: Spectroscopic characterization upon activation and interaction with adsorbates. *Chemistry of Materials* **2006,** *18* (5), 1337-1346.

Sandia National Laboratories is a multi-program laboratory managed and operated by Sandia Corporation, a wholly owned subsidiary of Lockheed Martin Corporation, for the U.S. Department of Energy's National Nuclear Security Administration under Contract DE-AC04-94AL85000.